

## A SOLUTION TO CHARACTERISTICS OF PLANAR TRANSMISSION LINES MADE OF FINITE-THICKNESS METAL ON MULTI-LAYER MEDIA

J. C. Liou and K. M. Lau

Electrical and Computer Engineering Department  
University of Massachusetts  
Amherst, MA 01003

### ABSTRACT

When analyzing signal transmission characteristics of metal lines on semiconductor devices and circuits, the assumption that metal is perfectly conducting is not always valid. In this paper, a simple, accurate way to include metallic loss in spectral domain analysis of planar transmission lines built on multi-layer semiconducting media is presented. Applications to analyzing IC interconnection delays, calculating FET gate electrode losses and optimizing monolithic slow-wave devices are also described.

### INTRODUCTION

There is a great amount of interest in analyzing the characteristics of metallic interconnecting lines on semiconductor wafers. Large amount of time delay, dispersion and attenuation may occur if the media underneath is not lossless, due to limited electric field penetration. There exist several approaches of analysis, such as quasi-TEM, spectral-domain analysis (SDA) and the finite-element method. The SDA method is particularly versatile in analyzing integrated circuit-related structures because irregularly shaped geometries are relatively easy to implement. New device concepts and integration schemes have made the vertical composition of an integrated circuit more complicated. Thus when the spectral-domain method is used, the formulations for the Green's functions need to include as many layers of media (lossy and lossless) as possible.

Several SDA approaches that can handle the complexity of nowadays integrated circuit exist [1,2]. However, one aspect of the problem frequently neglected is the fact that in semiconductor device fabrication, the thickness of metal deposited may be comparable to the skin depth of the metal. The "perfectly conducting" assumption becomes questionable. For instance, the thickness of 1  $\mu\text{m}$  gold is less than half of a skin depth at 1 GHz. Even for higher frequencies where metal thickness becomes as large as several times of a skin depth, the surface resistance can always contribute to time delay and attenuation. Most of the existing work addressing this issue utilizes quasi-static or finite-element solutions.

In this paper, a solution based on a SDA approach to find the propagation constant of a planar transmission line built on multi-layered, isotropic media, and made of finite-thickness metals will be presented. Calculated results are

comparable to experimental ones. The transmission line types include microstrip and coplanar waveguide. Since this approach can fully describe the transmission characteristics over a wide range of frequencies, some interesting applications emerge. These applications will be described briefly.

### MODEL DEVELOPMENT

It is desirable to use the imittance approach [2] in this solution due to its easiness to handle multi-layer media. First let us designate the region above the metal strip as region 1 and the region below as region 2. Region 2 can include several layers of uniform lossless or lossy materials. Figure 1 shows the equivalent transmission lines for both TE and TM fields when they are decomposed in the  $(u, v)$  coordinate system [2]. Quantities with the " $\sim$ " are the Fourier transforms of corresponding quantities without it. Taking the TM-to- $y$  equivalent circuit as an example, if the metal strip is perfectly conducting, the boundary conditions at  $y=0$  are

$$\tilde{H}_{u1} - \tilde{H}_{u2} = \tilde{J}_v, \quad \tilde{E}_{v1} = \tilde{E}_{v2} = \tilde{E}_v \quad (1)$$

$$\frac{-\tilde{H}_{u1}}{\tilde{E}_{v1}} = Y_1^e, \quad \frac{\tilde{H}_{u2}}{\tilde{E}_{v2}} = Y_2^e \quad (2)$$

Here  $Y_1^e$  and  $Y_2^e$  are admittances looking up and looking

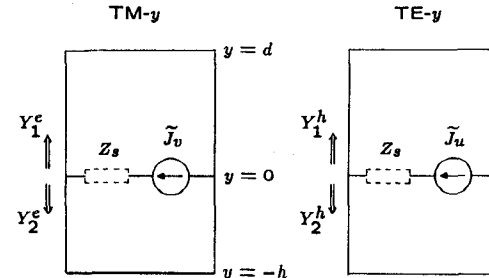
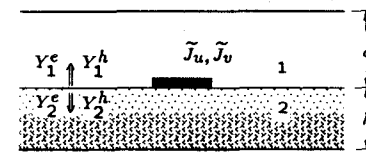


Figure 1. Equivalent transmission lines for the TM and the TE fields.  $Z_s$  is included when metal loss of the strip is taken into account.

down from the source  $\tilde{J}_v$ , respectively. When these admittances are evaluated, semiconductor layers can be handled by including its conductivity  $\sigma_s$  as an imaginary part of the relative permittivity  $\epsilon_r$ ,

$$\epsilon_r' = \epsilon_r - j \frac{\sigma_s}{\omega}. \quad (3)$$

To consider actual metals, we have to realize that

1. The metal has finite conductivity;
2. the metal is of finite thickness; and
3. the current distributes unevenly within the cross-section of the metal, with the tendency that the current density is higher at the surface and at corners.

For many cases of interest in semiconductor circuitries, where linewidths are much smaller than a wavelength, it suffices to reformulate (2) as

$$\frac{\tilde{H}_{u2} - \tilde{H}_{u1}}{\tilde{E}_v + Z_s \tilde{J}_v} \approx Y_1^e + Y_2^e. \quad (4)$$

Here  $Z_s$  is the surface impedance of the metal and the term  $Z_s \tilde{J}_v$  reflects the tangential electrical fields in the strip region. Equation (4) can be re-written as

$$\tilde{E}_v \approx -(Z^e + Z_s) \tilde{J}_v \quad (5)$$

where  $Z^e = (Y_1^e + Y_2^e)^{-1}$ . The case for the TE fields is found in a similar way and we have

$$\tilde{E}_u \approx -(Z^h + Z_s) \tilde{J}_u \quad (6)$$

where  $Z^h = (Y_1^h + Y_2^h)^{-1}$ . From (5) and (6) we recognize the surface impedance as the "internal impedance" of the driving current elements in the equivalent transmission line circuit, as was shown in Figure 1. Now since  $E$  and  $J$  are mutually exclusive in space domain along the  $x$  axis, the rest of the Galerkin's procedure in Fourier transformed domain can proceed.

The surface impedance as a function of thickness,  $t$ , and conductivity,  $\sigma$ , of the metal is given by [3]

$$Z_s = R + j\omega L; \quad (7)$$

where

$$R = \frac{1}{\delta\sigma} \left[ \frac{\sinh(2t/\delta) + \sin(2t/\delta)}{\cosh(2t/\delta) - \cos(2t/\delta)} \right] \quad (8)$$

$$\omega L_i = \frac{1}{\delta\sigma} \left[ \frac{\sinh(2t/\delta) - \sin(2t/\delta)}{\cosh(2t/\delta) - \cos(2t/\delta)} \right] \quad (9)$$

and  $\delta = (2/\omega\mu\sigma)^{1/2}$  is the skin depth. Note that  $t$  can assume any value. The characteristics of  $Z_s$  differ sharply between the cases of  $t > \delta$  and  $t \ll \delta$ . For the former case,  $R \approx \omega L_i$ . But for the latter, the value of  $R$  dominates.

When the thickness-to-width ratio  $t/w$  is close to one, surface loss at side walls of the metal can not be ignored, particularly at higher frequencies. Surface roughness can also give rise to additional loss. We empirically include these factors as a multiplying factor  $F_L (> 1)$  to  $Z_s$ . This is equivalent to a slight increase in the internal impedance.

## MODEL VERIFICATION

Numerical calculations were first carried out for MOS coplanar waveguide slow-wave structures in [4] for which a quasi-TEM model suffices. Excellent agreements are found. In Figure 2, an  $n - n^+$ -layer loaded slow-wave structure is analyzed. In this case, since  $t/w$  is close to 1,  $F_L$  as large as 1.5 is used at the highest frequency (20 GHz). The present method evidently provides closer estimation of phase and attenuation constants than earlier calculations ignoring the multilayer nature and metal losses [5].

## POTENTIAL APPLICATIONS

Since the present model takes into account most aspects of physical properties of a transmission line structure, it gives a more accurate estimation of characteristics over a wider range of frequencies than a quasi-TEM model can provide. The capability to handle multilayer structures also implies that more categories of circuitries can be applied. Three areas are found to have potential applications.

### Monolithic Slow-Wave Device Characteristics

Ideal slow-wave devices fabricated on semiconductor substrates opt for large phase shift with low loss. If the figure of merit of these devices is defined as the ratio of slow-wave factor ( $\lambda_0/\lambda$ ) to unit length attenuation, we can optimize this figure of merit using structural parameters. For example, in Figure 3, the figure of merit of the device analyzed in Figure 2 is shown for a wide variety of other possible choices. If low characteristic impedance can be tolerated, designs labeled C, E and I give the best figure of merit.

### FET Gate Finger Propagation

Another interesting application of this new method is to estimate the end-to-end signal degradation of gate electrodes in MESFETs and MODFETs [6]. In Figure 4, a typical MODFET with 1  $\mu\text{m}$  gate length is analyzed for signal transmission characteristics along the gate finger. The estimated high values of slow-wave factor and attenuation constant could limit the MODFET's power handling capability. As an example, if the gate electrode has a width of 200  $\mu\text{m}$ , then the end-to-end  $S_{21}$  equals .71L-45 ( $Z_0 = 50\Omega$ ) at 6 GHz. The far end may contribute very little, if not adversely, to power amplification.

### IC Interconnection Delay

For most digital IC designs, long interconnection lines are common. These lines are fabricated on top of a layer of insulator and possibly with semiconductor active layers underneath. Slow-wave phenomena will possibly occur. Figure 5 shows an example for a typical GaAs digital IC. The time waveforms are obtained through frequency-domain analysis. Rise time and propagation delay can be found from these waveforms. It is evident that critical timing requirement can be satisfied by carefully choosing structural parameters.

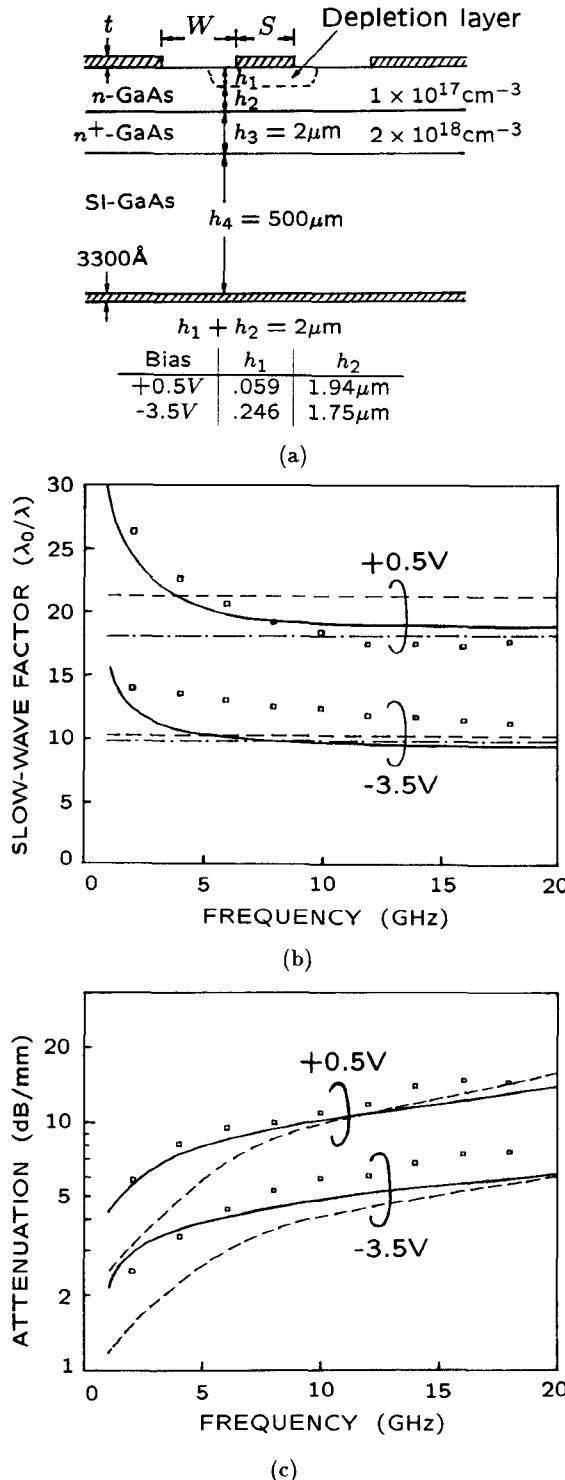


Figure 2. Analysis of an  $n - n^+$ -layer loaded Schottky contact slow-wave structure, biased at  $+0.5V$  and  $-3.5V$ . (a) Cross-sectional view. Here  $S = 1.5 \mu\text{m}$ ,  $W = 5 \mu\text{m}$ ,  $t = 6300 \text{ \AA}$ , metal conductivity =  $4.1 \times 10^5 \text{ S/cm}$ . (b) Slow-wave factor. Measurement (□), transport analysis (----), full-wave field analysis (—), all by [5]; and present method (—). (c) Attenuation. Measurement (□), transport analysis plus quasi-static estimation (—), both by [5]; and present method (—).

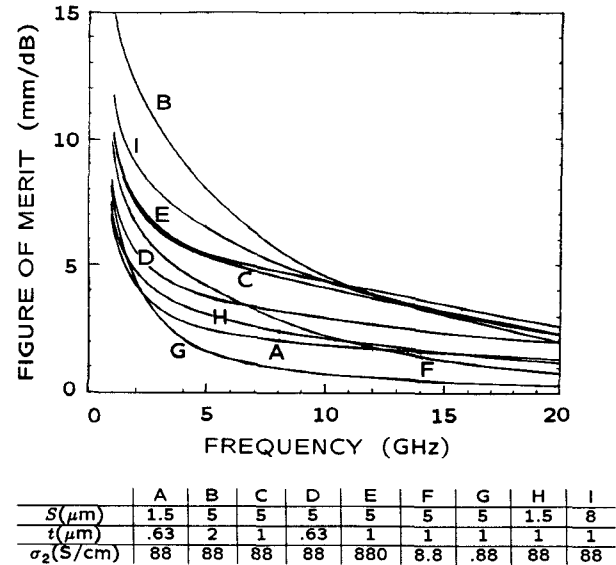


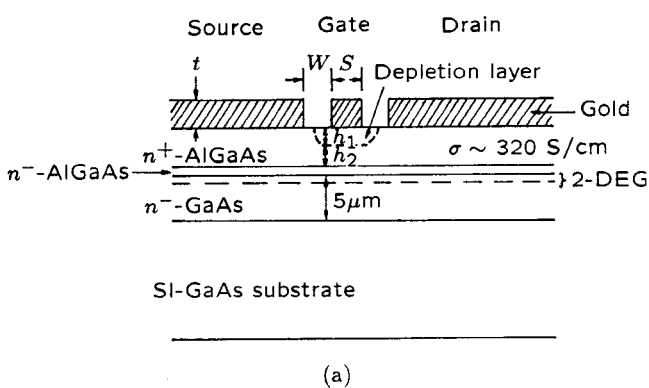
Figure 3. Figure of merit for variations of the structure in Figure 2.  $W = 5 \mu\text{m}$  is used throughout all cases. Case A is the condition used in Figure 2. Here  $\sigma_2$  represents the conductivity for the  $n$ -GaAs layer.

## CONCLUSIONS

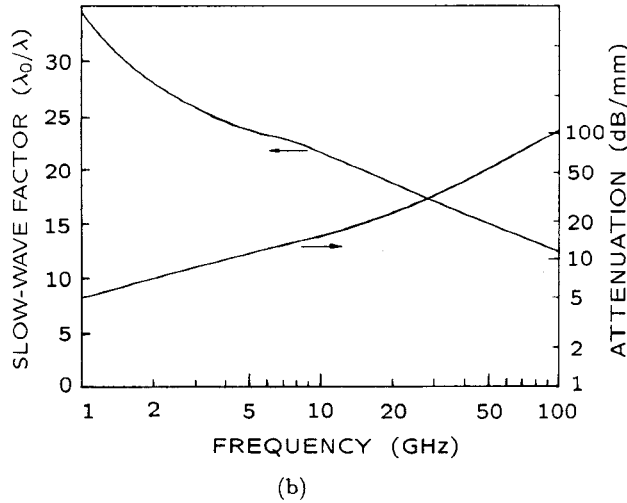
To conclude, we have implemented an easy way to include metallic loss in spectral domain analyses of planar transmission lines with complicated semiconducting medium layers. This approach provides accurate evaluations of properties of metallic lines for a wide range of high speed and high frequency semiconductor circuitries.

## ACKNOWLEDGEMENTS

This work was supported by NSF grant No. ECS-8708259. The authors wish to thank Dr. Robert W. Jackson and Dr. Nirod K. Das for their useful suggestions.

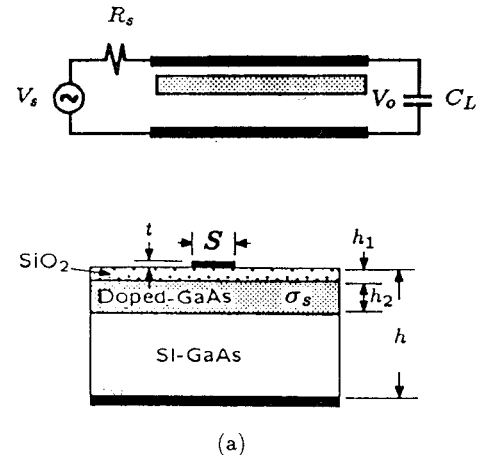


(a)

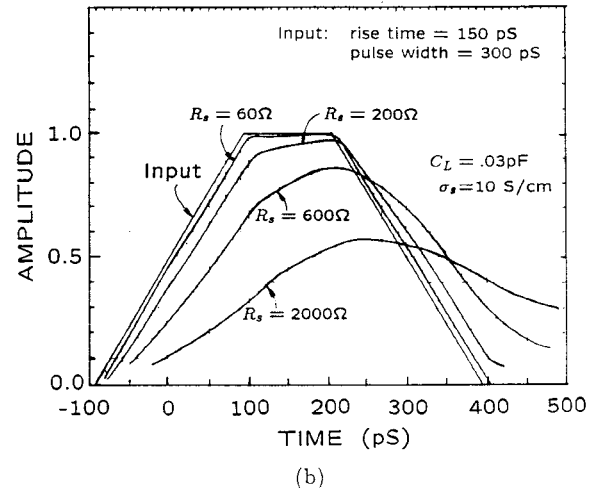


(b)

**Figure 4.** Analysis of the gate electrode of a typical MODFET. (a) Cross-sectional view. Here  $S = W = t = 1\mu\text{m}$ ,  $h_1 = 250\text{\AA}$ ,  $h_2 = 350\text{\AA}$ . For 2-DEG, we assume a sheet electron density of  $1 \times 10^{12}\text{cm}^{-2}$  and is approximated by a uniform layer with thickness of  $100\text{\AA}$  and  $\sigma = 1280\text{ S/cm}$ . (b) Calculated slow-wave factor and attenuation.



(a)



(b)

**Figure 5.** (a) A sample interconnect circuit and the cross-sectional view of the media under the interconnect line. (b) Input/output time waveforms. Here  $t = 5000\text{\AA}$ ,  $S = 1.5\mu\text{m}$ ,  $h_1 = 2500\text{\AA}$ ,  $h_2 = 2500\text{\AA}$ ,  $h = 200\mu\text{m}$ . The metal for the line is gold. The line length is  $500\mu\text{m}$ .

## REFERENCES

- [1] Das, N. and D. Pozar, "A Generalized Spectral-Domain Green's Function for Multilayer Dielectric Substrates with Application to Multilayer Transmission Lines," *IEEE Trans. Microwave Theory Tech.*, Vol. MTT-35, pp. 326-335, March 1987.
- [2] Itoh, T., "Spectral Domain Immitance Approach for Dispersion Characteristics of Generalized Printed Transmission Lines," *IEEE Trans. Microwave Theory Tech.*, Vol. MTT-28, pp. 733-736, July 1980.
- [3] Ramo, S., J. Whinnery, and T. V. Duzer, *Fields and Waves in Communication Electronics*, page 301, John Wiley & Sons, Inc., New York, 1965.
- [4] Kwon, Y., V. Hietala, and K. Champlin, "Quasi-TEM Analysis of 'Slow-Wave' Mode Propagation on Coplanar Microstructure MIS Transmission Lines," *IEEE Trans. Microwave Theory Tech.*, Vol. MTT-35, pp. 545-551, June 1987.
- [5] Krown, C. and G. Tait, "Propagation in Layered Biased Semiconductor Structures Based on Transport Analysis," *IEEE Trans. Microwave Theory Tech.*, Vol. MTT-37, pp. 711-722, Apr. 1989.
- [6] Seguinot, C., P. Kennis, P. Pribetich, and J. Legier, "Analytical Model of the Shottky Contact Coplanar Line," In *Proc. 14th Euro. Microwave Conf.*, pages 160-165, Liege, 1984.